JOURNAL OF COMPUTATIONAL PHYSICS 119, 94–104 (1995)

Particle Simulation of Complex Flows in Dilute Systems

F. BARAS AND M. MALEK MANSOUR

Université Libre de Bruxelles, Center for Nonlinear Phenomena and Complex Systems, Campus Plaine, CP 231, B-1050 Brussels, Belgium

A. L. GARCIA*

Institute for Scientific Computing Research, Lawrence Livermore National Laboratory, Livermore, California 94550

AND

M. MARESCHAL

Université Libre de Bruxelles, Center for Nonlinear Phenomena and Complex Systems, Campus Plaine, CP 231, B-1050 Brussels, Belgium

Received February 22, 1994; revised November 16, 1994

The direct simulation Monte Carlo (DSMC) algorithm, introduced in 1976 by G. A. Bird, proves to be extremely efficient for simulating dilute gas flows. However, due to the relatively large transport coefficients at low densities, a high Rayleigh or Reynolds number is difficult to achieve by this technique. We present a modified version of DSMC in which the relaxation processes are enhanced and the transport coefficients reduced. This is achieved by increasing the ratio between collisions and free flow of particles in a suitable way. The modified algorithm is mostly useful for statistical physics applications, since it leads to the correct fluctuation spectrum. Several computational experiments are described; they demonstrate that the correct equilibrium and nonequilibrium fluid properties are preserved. The new algorithm is shown to be significantly more efficient than molecular dynamics for simulating complex hydrodynamical flows.

1. INTRODUCTION

With the development of high speed computers, much attention has been focused in the past decade on the microscopic simulation of non-equilibrium hydrodynamic systems [1, 2, 3]. For example, complex phenomena such as shock waves [4], flow past an obstacle [5], and hydrodynamic instabilities [6, 7] have been successfully simulated through molecular dynamic (MD) simulations. The next challenge is obviously the microscopic simulation of high Reynolds number flows, a domain where the wealth of theoretical speculations contrasts with the difficulties in obtaining precise experimental results [8]. Unfortunately, traditional MD simulation of high Reynolds number flows still seems beyond the reach of present day computers.

One approach to overcome this difficulty is to simplify as much as possible the underlying microscopic dynamics and, possibly, to reduce the dimension of the embedding space. A well-known example is the hard disk fluid that has been used for the simulation of two-dimensional Rayleigh–Bénard instabilities [6, 7]. Recently, Rayleigh numbers as high as 80,000 have been reported in simulations of 50,000 hard disks [9]. In these systems, a secondary bifurcation that leads to periodic behavior of convective rolls has been observed. A single run of such a simulation requires about 15 days of CPU time on an IBM 3090 supercomputer. A rough estimate shows that reaching the turbulence regime would require about 10 times more particles and over six months of CPU time.

Another possibility is to consider dilute systems in the Boltzmann limit since there exist efficient algorithms, like the Bird algorithm [10], usually referred to as DSMC (direct simulation Monte Carlo), which are typically three orders of magnitude faster than comparable MD simulations. In this case, however, one has to face two new difficulties.

First, one is typically interested in simulating strictly subsonic flows, for otherwise the shock waves generated in the system make the analysis and the theoretical interpretation of the results extremely difficult. The Reynolds number is proportional to the mean flow velocity and it is therefore limited by the value of the sound speed. Since the latter is about three times smaller in dilute gases than in liquids, the maximum possible value of the Reynolds number in subsonic flows remains also about three times smaller in dilute gases and there seems to be no way to increase this ratio.

A second and perhaps more serious difficulty arises from the fact that the transport coefficients of dilute gases are significantly larger than those of dense fluids. This is shown in Fig. 1, where the density dependence of the kinematic viscosity ν of hard sphere fluids is depicted. The shape and the order of

* Permanent address: Dept. Physics, San Jose State University, San Jose, CA 95192.

0021-9991/95 $6.00

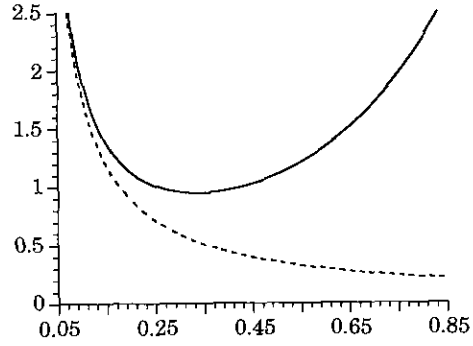

FIG. 1. Kinematic viscosity versus number density. The solid line corresponds to hard sphere Enskog gas, whereas the dashed line represents the Boltzmann values extrapolated to high densities (cf. Section 6).

magnitude is roughly the same for any other short range binary interaction potential, such as the Lennard–Jones potential. Note that the length unit is the sphere diameter d, a scale unit used throughout the paper. As can be seen from Fig. 1, the kinematic viscosity goes through a minimum at a number density of about 0.3 which corresponds to a relatively dense Enskog gas (in this case the particles occupy about 15% of the volume of the system). Since the Reynolds number is inversely proportional to the kinematic viscosity, the best strategy in simulating high Reynolds number flows is to choose a number density close to 0.3, which is far beyond the validity of the Boltzmann equation. As a matter of fact, the Boltzmann equation holds only for number densities smaller than 6×10^{-3}, in which case the corresponding kinematic viscosity is more than 30 times larger than this minimum value [10]. Note that the number density for air is 1.33×10^{-3} at standard atmospheric conditions.

This last problem is a serious handicap that clearly limits the usefulness of the DSMC method in simulating high Reynolds number flows, unless one can find a way to modify the values of the transport coefficients. In other words, the question arises: *is it possible to set up an algorithm allowing the simulation a fluid with adjustable transport coefficients, while remaining strictly within the Boltzmann limit?* The main purpose of this paper is to show that, indeed, such an algorithm can be constructed.

At this stage one could ask whether it is not worth simplifying the microscopic dynamics even further and consider, for example, the lattice gas cellular automata (LGCA) or the lattice Boltzmann (LB) method, that, indeed, allow the simulation of relatively high Reynolds number flows [11] and other instabilities [12, 13]. The answer depends on the type of questions one wants to clarify through microscopic simulations. Our main interest is to use microscopic simulations as an "experimental" tool to check the validity of theoretical approaches or to account for cases where high-precision laboratory experiments are difficult or impossible to perform. To this end, we need a method whose validity goes beyond that of macroscopic hydrodynamics, and which is also able to reproduce the correct fluctuation spectrum. This last requirement is crucial, since most of the existing theories about turbulence are essentially statistical theories [14]. So far it is not clear whether the LGCA or the LB method contains more information than the macroscopic Navier–Stokes equations [15].

The Bird algorithm, on the other hand, fully satisfies all the above requirements: it agrees with all the experimental data concerning rarefied gas dynamics, including peculiar situations where hydrodynamics fail; it is in perfect agreement with Landau–Lifshitz fluctuating hydrodynamics, even in extreme nonequilibrium conditions [16]; it reproduces correctly the data obtained through hard-sphere molecular dynamics in strong shock wave conditions (Mach number >100), a domain far beyond the validity of Navier–Stokes equations [17].

The paper is organized as follows. In Section 2 we outline the basic elements of the standard DSMC method and present the main ideas at the basis of our enhanced-relaxation variant. To check the validity of this new algorithm, we consider three different computer experiments. The first, Poiseuille flow, allows a direct measurement of the kinematic viscosity through the velocity profile; it is described in Section 3. In Section 4, we study the statistical properties of an equilibrium system by measuring the dynamic structure factor. The latter is compared with its theoretical expression, obtained using the Landau–Lifshitz fluctuating hydrodynamics [18]. In order to check the validity of the enhanced-relaxation algorithm in the presence of hydrodynamic instabilities, Section 5 discusses the Bénard problem and the comparison with results obtained using macroscopic hydrodynamics. In Section 6 we estimate the relative computational efficiency of the enhanced-relaxation Bird algorithm versus molecular dynamics. Concluding remarks and perspectives are presented in Section 7.

2. ENHANCED-RELAXATION BIRD ALGORITHM

Some 20 years ago, G. A. Bird proposed his now famous DSMC algorithm to simulate the Boltzmann equation. The original purpose of the method was to deal with problems where the use of the standard hydrodynamic descriptions, such as the Navier–Stokes equations, becomes questionable. A common application of the method is the computation of high Knudsen number flows of a rarefied gas past an object (e.g., high altitude flight). Bird's method has become popular since it is in excellent agreement with experimental and numerical data.

The algorithm we shall discuss is based on the traditional DSMC [10], whose basic steps can be summarized as follows: As with usual molecular dynamic methods, the state of the system is the set of particle positions and velocities, $\{\mathbf{r}_i, \mathbf{v}_i\}$, $i = 1, \ldots, N$, where N is the total number of particles. The evolution of the system is integrated in time steps Δt, typically a fraction of the mean collision time for a particle. Within a time step, the free flight motion and the particle interactions (collisions) are assumed to be decoupled. The free flight motion for each particle i is computed as $\mathbf{r}_i(t + \Delta t) = \mathbf{r}_i(t) + \mathbf{v}_i(t)$

Δt, along with the appropriate boundary conditions. After all the particles have been moved, they are sorted into spatial cells, typically a fraction of a mean free path, λ, in length. Each cell is assumed to be perfectly homogeneous, i.e., all particles within a cell are considered to be candidate collision partners, regardless of their exact positions. This major hypothesis allows one to consider, during the time step Δt, a "homogeneous" Boltzmann equation within each cell.

The theory underlying the simulation of the homogeneous Boltzmann equation was first proposed by Kac [19] who assumed that the collisional process can be described as a "*jump Markov process.*" With this hypothesis, the probability of the collision for a pair of hard-sphere particles is directly proportional to the modulus of their relative speed and the waiting times between collisions are exponentially distributed. The computational cost of evaluating waiting times increases very rapidly with the number of particles, so that Bird proposed an interesting alternative. It consists of evaluating these waiting times by dividing an estimate of the average distance of colliding particles by the modulus of their relative speed.

A set of representative collisions, for the time step Δt, is chosen in each cell. For each selected pair a random impact parameter is generated and the collision is performed. Note that linear momentum and energy are conserved in the evaluation of the collision, whereas the angular momentum is only conserved on average. After the collision process has been completed in all the cells, the particles are moved according to their updated velocities and the procedure is repeated as before.

The resulting velocity distribution function obeys a Boltzmann-like equation [20]

$$(\partial_t + \mathbf{v} \cdot \nabla) f(\mathbf{v}, \mathbf{r}, t) = B(ff'), \tag{1}$$

where B represents a "model" collision operator. Since the free flight motions of the particles are computed exactly, the left-hand side of (1) is exact. As a consequence, the non-dissipative parts of the resulting hydrodynamic equations are also exact. The nature of the dissipative terms, on the other hand, depends directly on the way the collision processes are modeled. Since B conserves energy and linear momentum, these dissipative parts are necessarily in the form of the divergence of a dissipative flux. Therefore, no matter how B is modeled, the general structure of the hydrodynamic equations is preserved. Remarkably, the Bird algorithm also gives the correct transport coefficients, as predicted by Chapman–Enskog theory [21] and the correct fluctuation spectrum, as given by Landau–Lifshitz fluctuating hydrodynamics.

Suppose now that we modify B, while preserving its conservation properties. The resulting hydrodynamics will still be correct, except for the fact that the transport coefficients will no longer agree with their Boltzmann expressions. We shall take advantage of this in the following way.

The values of the transport coefficients in dilute gases are directly related to the balance between two processes: collisions and free flights. During the collision step, the velocity distribution approaches locally a Maxwellian distribution. The free flight motions of the particles, on the other hand, destroy this local Maxwellian. These conflicting processes determine the "relaxation time" τ of the system. The viscosity of the fluid is directly proportional to this relaxation time as

$$\nu \approx \tau k_B T, \tag{2}$$

where k_B and T are Boltzmann's constant and temperature, respectively; the thermal diffusivity coefficient obeys a similar relation. Note that in dilute gases, the relaxation time is also a function of the local temperature.

Now suppose that we increase the time step used for the collisions by a scaling factor S_c, while keeping it unchanged for the free flight step. The local velocity distribution function will then be S_c times "closer" to its local equilibrium value and, in turn, the resulting relaxation time and transport coefficients will also be S_c times smaller than their Boltzmann values. Of course, the effective time step allowed for the collisions ($S_c \Delta t$) cannot exceed the mean collision time per particle, since otherwise a given particle will experience, on average, more than one collision per time step. To be consistent, we must therefore choose an integration time step S_c times smaller than its normal value, which in turn increases the CPU time of the program by a similar amount. Moreover, since the mean free path λ is proportional to the relaxation time, decreasing the latter is equivalent to decreasing the former. In other words, we need more accurate spatial resolution, which can be achieved by dividing the length of the cells by S_c; that in turn requires more memory space for the program. These are the prices to be paid for this algorithm to be meaningful. Nevertheless, the "enhanced-relaxation" Bird algorithm still remains much faster than MD in comparable situations, as will be shown in Section 6.

Very recently, Bird proposed several modifications to DSMC that improve the performance and the flexibility of his original algorithm [22]. In particular, the new DSMC contains a parameter that allows one to set the "effective number of molecules" represented by each particle in the simulation. Increasing this number also decreases the transport coefficients so that, as far as macroscopic behavior of the fluid is concerned, this achieves straightforwardly the same goal as our algorithm. The use of an effective number for particles does not, however, preserve the statistical properties of the simulated fluids. For instance, let N be the number of particles inside a volume ΔV. It is well known that at thermodynamic equilibrium, the distribution of N is Poissonian so that mean square deviation of N is simply equal to its average value, i.e., $\langle \delta N^2 \rangle = \langle N \rangle$. If now we use the concept of "effective number" and say that each simulated particle represents M real atoms, then $\langle \delta(M N)^2 \rangle = M^2 \langle N \rangle$, whereas the correct mean square deviation is $M \langle N \rangle$. The main reason for this apparent discrepancy is related to the fact that fluctuations of extensive quantities, such as energy or number

of particles, do not scale as N but, as $N^{1/2}$, at least for near equilibrium fluids. As the fluid is driven through an instability, the scaling law of fluctuations changes and one of our main goals in the future is precisely to study the behavior of fluctuations in turbulent regimes through particle simulation. The algorithm we present simply enhances the relaxation toward local equilibrium without changing the fluid density and, hopefully, it will preserve the statistical properties of the fluid.

To sum up, we consider the traditional DSMC method, where we introduce a new parameter S_c. The duration of each collision is then simply reduced by S_c. As a result, the program performs, on average, S_c times more collisions than it would in normal DSMC method. Since the free-flight processes are unchanged, we have to consider S_c times more collisional cells in each spatial direction and reduce the integration time step by the same amount. Everything else remains exactly the same as in the usual DSMC.

The theoretical arguments to justify the validity of the enhanced-relaxation Bird algorithm, although highly plausible, are nevertheless heuristic and need to be carefully tested. Specifically, we should check whether the equilibrium properties (e.g., equation of state, the speed of sound), the hydrodynamics and the fluctuation spectrum are correctly preserved in this new algorithm. The next three sections present a series of computer experiments which test the DSMC algorithm and its enhanced-relaxation variant for hard-sphere fluids. For practical convenience, lengths and masses are scaled by the sphere diameter d and the particle mass m, respectively, i.e., we take $d = m = 1$. Similarly, by an appropriate scaling of time and velocities, the equilibrium (reservoir) temperature and thermal velocity are set to unity. In these units, the Boltzmann constant is equal to 0.5. In all cases, the global number density (total number of particles divided by the volume of the system) will be set equal to 5.34×10^{-3}, which corresponds to 400 particles per cubic mean free path, when $S_c = 1$.

3. POISEUILLE FLOW

We start with the microscopic simulation of plane Poiseuille flow, also known as channel flow. Consider an assembly of N particles confined between two rigid, parallel plates located at $y = 0$ and $y = L$. These plates are stationary and act as infinite thermal reservoirs, i.e., each time a particle strikes one of them, it is re-injected into the system after having its velocity reset according to a half-Maxwellian distribution at the reservoir temperature $T_R = 1$. Periodic boundary conditions are assumed in the other two directions and a constant acceleration field, g, oriented in the x direction is applied to the system.

Assuming the flow is laminar, at the stationary state the x-component of the velocity field is a parabolic function of the y-coordinate:

$$\mathbf{v} = \frac{g}{2\nu} y(L - y)\mathbf{1}_x + u_s \mathbf{1}_x, \tag{3}$$

where $\mathbf{1}_x$ is the unit vector in the x direction and u_s represents the velocity slip at the walls. From the average velocity profile, one can directly measure the kinematic viscosity, ν.

It should be noted that in deriving (3) we have assumed that ν is constant. For a Boltzmann hard-sphere gas, however, the viscosity coefficient is proportional to $\sqrt{T}$. Assuming constant pressure, the density is inversely proportional to T. As a result, ν is inversely proportional to $\sqrt{T}$ and, because of energy dissipation, the temperature is not uniform throughout the system (viscous heating). In fact, neglecting the temperature dependence of ν and thermal diffusivity coefficient λ_T, the temperature profile is given by

$$T = T_R + \frac{g^2}{12\, c_v \nu \lambda_T}\left[\left(\frac{L}{2}\right)^4 - \left(\frac{L}{2} - y\right)^4\right], \tag{4}$$

where c_v is the heat capacity at constant volume. In principle, this expression can be used to measure directly the thermal diffusivity coefficient as well, as it has been done for dense fluids [23]. For dilute gases, however, this procedure is quite difficult to set up, mainly because the amplitude of $T(y)$, as compared to the reservoir temperature, is generally quite small (it is proportional to the square of the velocity gradient). To get reasonable statistical accuracy (signal to noise ratio), one has to consider a relatively large value of the acceleration field g, but then the temperature dependence of transport coefficients can no longer be neglected. There are also other problems, mainly related to the temperature jump and noise at the boundaries, so that in this section we will concentrate on the kinematic viscosity.

For the simulation we use $N = 2000$ particles and 40 collisional cells in the y direction with $L = 421.56\, d$ (=10 mean-free paths). We first consider the standard DSMC, i.e., $S_c = 1$, and take $g = 1.2 \times 10^{-4}$. With this choice of parameters, the variation in the temperature profile does not exceed 0.2% so that the temperature dependence of transport coefficients can indeed be neglected. The system is also divided into 20 statistical cells in y direction. In these cells, a space averaging is performed to give instantaneous values of the conserved mechanical quantities: mass, momentum, and energy density. A time averaging then leads to the local macroscopic quantities, such as temperature, velocity, etc. The total run executed about 10^6 collisions per particle (CPP). The statistical errors, estimated over successive intervals of 10^5 CPP, do not exceed 0.8%. The theoretical value of the kinematic viscosity for the above set of parameters is 23.35; the measured value is found to be 23.3 ± 0.1, in excellent agreement with the theory.

To test our enhanced-relaxation algorithm, we next consider the same simulation, but with $S_c = 10$. The expected kinematic viscosity should now be 10 times smaller than its Chapman–Enskog value. The system is divided into 400 collisional cells (5 particles per cell) and 40 statistical cells. The best way to test the theory is to choose an acceleration field $g = 1.2 \times$

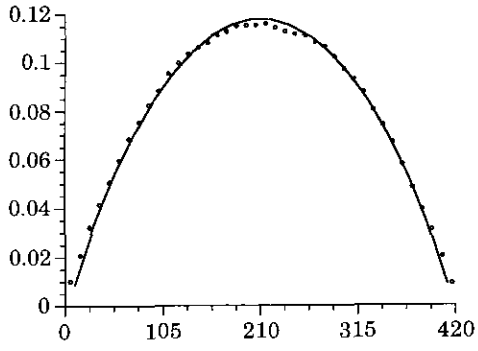

FIG. 2. Measured velocity profiles. The solid line represents the results obtained using the standard Bird algorithm ($S_c = 1$), with $g = 5 \times 10^{-3}$, whereas the dots correspond to the enhanced-relaxation algorithm ($S_c = 10$) with $g = 5 \times 10^{-4}$. In each case, the velocity slip has been removed.

10^{-5} (10 times smaller than its previous value), since then the velocity profile should remain unchanged (see Eq. (3)).

Our first observation concerns the velocity slip at the boundaries. According to elementary kinetic theory, one has [24]:

$$u_s = 2C\lambda(\partial v_x/\partial y)_{\text{wall}} \tag{5}$$

where C is a numerical constant whose value is about 0.491. Since transport coefficients are proportional to the mean free path, λ, we expect a velocity slip 10 times smaller than in the previous (normal) case; this is precisely what is observed.

Next, we consider the velocity profiles shown in Fig. 2. In each case, the velocity slip has been removed. As can be seen, there is very good agreement between the two results, although the statistical errors are larger for $S_c = 10$ than for $S_c = 1$. As we already mentioned, to get the same statistical accuracy, the total running time of the program must be 10 times larger for the former than for the latter case. Here, however, we have chosen the same total computation time for both simulations (10^6 CPP). As a result, the estimated statistical error is about 3% for $S_c = 10$.

These results clearly show that the enhanced-relaxation algorithm accurately reduces the kinematic viscosity by a factor of $1/S_c$. Next, we show that the thermodynamic properties and the fluctuation spectrum of the fluid are preserved as well in the simulations.

4. DYNAMIC STRUCTURE FACTOR

In this section we study the statistical properties of equilibrium systems. Specifically, we measure the density fluctuations in the fluid. These spontaneous fluctuations generate temperature (or entropy) fluctuations and pressure fluctuations. While the former dissipate slowly in time through heat modes, the latter give rise to sound waves which propagate rapidly throughout the system and eventually are damped through viscous modes. The study of density fluctuations yields important information about both the thermodynamic properties (equation of state, speed of sound, etc.) and the transport properties of the fluid.

For the simulations, we consider an assembly of $N = 3000$ hard spheres in a box with dimensions $L_x = 1264.7\ d\ (=30\ \lambda)$ and $L_y = L_z = 21.1\ d\ (= 0.5\ \lambda)$; periodic boundary conditions are used in all directions. The system is partitioned in the x direction into 60 collisional cells (which are also used as statistical cells). After the fluid has relaxed to equilibrium, statistics are taken over 10^6 CPP to measure the Fourier transform of Van Hove total correlation function, defined as [21]:

$$F_{\mathbf{q}}(t) = \langle n_{\mathbf{q}}(t) n_{-\mathbf{q}}(0)\rangle - |\langle n_{\mathbf{q}}\rangle|^2, \tag{6}$$

where $n_{\mathbf{q}}$ is the Fourier transform of the number density:

$$n_{\mathbf{q}}(t) = \frac{1}{\sqrt{N}} \sum_{\alpha} \exp\{i\mathbf{q}\cdot\mathbf{r}_\alpha\} N_\alpha(t). \tag{7}$$

Here, $N_\alpha(t)$ represents the instantaneous number of particles in the statistical cell "α" and $\mathbf{r}_\alpha$ is the position of that cell. Note that for $\mathbf{q} \neq 0$, the second term on the right-hand side of (6) is zero, if the average density profile is uniform in space and, therefore, it is generally omitted.

To improve the statistics, we set $q_y = q_z = 0$; that is, we restrict ourselves to the study of "reduced" variables defined as the spatial average over the y and z directions. Since the system is finite, the wave vector $\mathbf{q}$ can only take discrete values:

$$\mathbf{q} = q_x \mathbf{1}_x; \quad q_x = \frac{2\pi}{L_x} k, \quad k = 1, 2, \ldots . \tag{8}$$

In hydrodynamic regime the function $F_k(t)$, as defined in Eq. (6) but with the restriction (8), is related to the time correlation of density fluctuations in the fluid through

$$F_k(t) = \frac{1}{N}\left(\frac{V}{m}\right)^2 \frac{1}{L_x^2} \int_0^{L_x} dx \int_0^{L_x} dx' \cdot \exp\left\{ i \frac{2\pi}{L_x} k(x - x') \right\} \langle \delta\rho(x, t)\delta\rho(x', 0)\rangle, \tag{9}$$

where $\delta\rho$ is the (mass) density fluctuation. The small size of the system, constrains us to small values of k, since we wish to remain in the hydrodynamic regime (typically, $k = 1$ or 2).

We first consider the standard DSMC; that is to say, we take

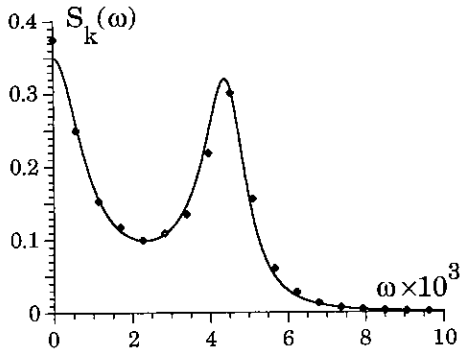

FIG. 3. Scattering function versus frequency for $k = 1$ measured in the Bird simulation using $S_c = 1$.

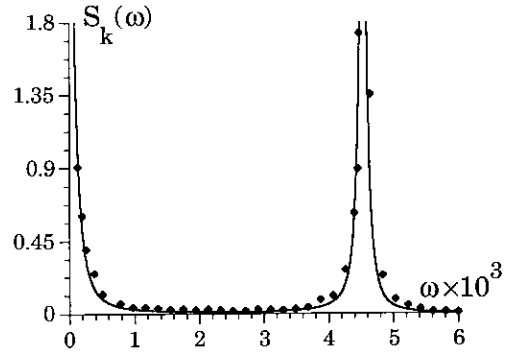

FIG. 4. Scattering function versus frequency for $k = 1$ measured in the Bird simulation using $S_c = 10$.

$S_c = 1$. Figure 3 shows the measured dynamic structure factor $S_k(\omega)$, also called the *scattering function*, defined as the time-Fourier transform of $F_k(t)$:

$$S_k(\omega) = \int_{-\infty}^{\infty} dt \exp\{i\omega t\} F_k(t). \tag{10}$$

The statistical error, estimated from successive runs of 10^5 CPP, does not exceed 8%, except for $\omega = 0$ (the long-time limit of $F_k(t)$), where it exceeds 20%. The theoretical expression of $S_k(\omega)$, as obtained from the Landau–Lifshitz fluctuating hydrodynamics [25], is also shown in the same figure. The peak near the origin is known as the Rayleigh line. Its width is directly proportional to the heat diffusivity coefficient. The second peak, known as the Brillouin line, is centered around $\omega = C_s 2\pi k/L_x$, where C_s is the sound speed (here, $k = 1$ and $C_s = 0.913$ in system units). The width of the Brillouin line is directly proportional to the kinematic viscosity. The total area under $S_k(\omega)$ allows one to estimate the compressibility coefficient of the fluid. The ratio of the area under the Brillouin peak and Rayleigh peak is equal to $c_p/c_v - 1$, where c_p represents the heat capacity at constant pressure. The very good agreement between the data and theory shows once more the accuracy of the DSMC method.

We next consider the enhanced-relaxation algorithm. Setting $S_c = 10$, we expect the transport coefficients to be lowered by an order of magnitude. The other parameters are as before, except that now we divided the system into 600 collisional cells in the x direction and use 300 cells to collect statistics. The program was run for 5×10^6 CPP (five times longer than in the previous case). In Figs. 4 and 5 we present the measured and theoretical scattering functions for $k = 1$ and $k = 2$, respectively. The estimated statistical errors are about 12% for $k = 1$ and 15% for $k = 2$. The parameters used in the evaluation of the theoretical scattering function are the same as in Fig. 3, except that the transport coefficients are divided by $S_c = 10$.

As can be seen, the agreement is very good, much better than the expected statistical errors. For instance, the measured speed of sound is 0.913 for $k = 1$ and 0.912 for $k = 2$, in excellent agreement with its theoretical value. The line shapes of the spectrum are also in very good agreement, showing that indeed all the thermodynamic and transport properties of the system are preserved by the enhanced-relaxation Bird algorithm. We have also measured the local velocity and temperature fluctuations and observed that the discrepancy with their theoretical values never exceed 5%.

In view of these results, there is no doubt that the enhanced-relaxation algorithm works perfectly in equilibrium and near equilibrium situations. As a final test, we next consider a far from equilibrium situations in the presence of a hydrodynamical instability, namely the Rayleigh–Bénard problem.

5. RAYLEIGH–BÉNARD INSTABILITY

In a fluid heated from below, the cold upper layers are heavier than the thermally expanded lower layers. This potentially unstable situation remains stable for small temperature gradients due to the dissipative effects of heat conduction and viscosity. However, above a critical value of the temperature gradient, the purely conductive state becomes unstable and a transition to well-structured convective behavior occurs. This transition, known as the Rayleigh–Bénard instability [26], is governed by the Rayleigh number R_a, defined as

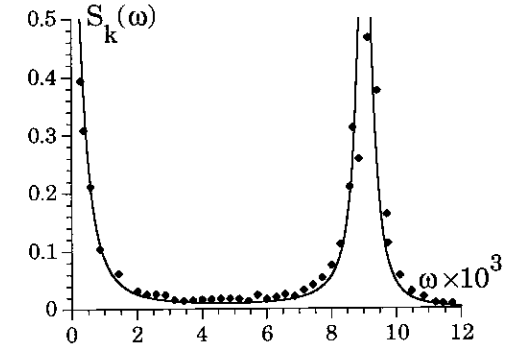

FIG. 5. Scattering function versus frequency for $k = 2$ measured in the Bird simulation using $S_c = 10$.

$$R_a = \frac{\alpha \Delta T g L_z^3}{\nu \lambda_T}, \tag{11}$$

where L_z is the distance between the horizontal plates, g the gravitational acceleration, and $\alpha = -(1/\rho)(\partial\rho/\partial T)_p$, the thermal expansion coefficient. The temperature difference, $\Delta T = T_L - T_U$, is the difference between the lower (T_L) and upper (T_U) plate temperatures. For stress-free boundary conditions, the critical value of the Rayleigh number is about 750.

For the simulation, we consider essentially a two-dimensional system by setting $L_x, L_z \gg L_y$. The fluid is subjected to an adverse external gravitational acceleration, g, in the z direction. Non-equilibrium constraints are imposed by stochastic horizontal walls which act as thermal reservoirs: each time a particle strikes the upper (lower) horizontal wall, it is re-injected into the system, conserving its tangential velocity component, while having its normal velocity component sampled from an equilibrium distribution at the upper (lower) wall temperature. This thermalisation mechanism simulates optimally stress-free boundary conditions [6]. The vertical sides are modeled as specularly reflecting walls. Macroscopically, this means insulating stress-free boundary conditions.

Microscopic simulations model extremely small systems. Since R_a is proportional to L_z^3, in order to overcome the instability threshold one has to apply an extraordinarily large temperature gradient and gravitational acceleration. These constraints, however, cannot be chosen arbitrarily large. For instance, if the gravity is excessively strong, the upper half of the system will be nearly empty. Furthermore, particle simulations become inefficient when the density gradient is large. One way to ensure a nearly uniform spatial distribution of particles, is to set

$$g = \frac{1}{\rho}\left(\frac{\partial p}{\partial T}\right)_\rho \frac{\Delta T}{L_z}. \tag{12}$$

We use this condition to fix the acceleration in all our simulations.

Finally, the temperature variation over a mean free path must be small if one is to remain within the hydrodynamic regime. In any case,

$$\frac{\Delta T}{\overline{T}} \leq 2, \tag{13}$$

where $\overline{T} = (T_L + T_U)/2$ is the average temperature. In practice, because of the temperature jump at the horizontal walls, the effective value of $\Delta T/\overline{T}$ is typically below 1.8. Note that this temperature jump is larger than it would be if both velocity components were thermalised [5] (corresponding to stick boundary conditions). But in this latter case the critical value of the Rayleigh number is more than two times larger than in the case of stress-free boundary conditions.

For the simulations we use $N = 40{,}000$ particles. The wall temperatures are set to $T_L = 1.5$ and $T_U = 0.5$, and the system size to $L_y = 42.156\ d\ (=1\ \lambda)$, $L_z = L_x = 421.56\ d\ (=10\ \lambda)$. For $S_c = 1$ (standard DSMC), one is below the convection threshold since the Rayleigh number is only 65.2. We use $S_c = 10$, so the Rayleigh number is about 6520, well above its critical value.

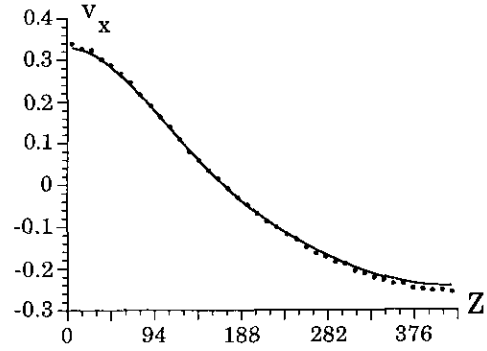

FIG. 6. Velocity profile of the horizontal velocity at ($x = L_x/2$) versus z for Rayleigh–Bénard convection. Solid circles are from Bird simulation with $S_c = 10$; solid line represents the solution of hydrodynamic equations.

The system is divided into 200×200 collisional cells (giving an average of one particle per cell). A space average is performed over 40×40 statistical cells to collect instantaneous values of basic mechanical quantities. After a short transient time of about 1000 collisions per particle (CPP), the system evolves to a single convective roll that remains stable for the rest of the run (210,000 CPP). After a relaxation period of 10,000 CPP, statistics are taken over 10 sequences of 20,000 CPP. This procedure allows an estimation of statistical errors; measured velocities and temperature are accurate to about 8%.

To verify our results, we compare them with those obtained from the Navier–Stokes equations. Because of the complexity of this problem (non-Boussinesq fluid, state dependent transport coefficients, mixed boundary conditions, etc.) we solve the full macroscopic hydrodynamic equations numerically using standard techniques [7]. For the equation of state we use the ideal gas law and for the transport coefficients we use the Chapman–Enskog expressions. To properly include the Knudsen layer (i.e., the temperature jump) into the hydrodynamic equations, we extrapolate the temperature profile measured in the simulation to obtain the "corrected" wall temperature. The extrapolated lower and upper wall temperatures are found to be 1.456 and 0.568 (as compared with 1.5 and 0.5).

Figures 6 and 7 illustrate the x-component of the velocity profile versus z and x, respectively. The convective velocity profiles measured in the enhanced-relaxation Bird simulation are in excellent agreement with hydrodynamic theory. The resulting temperature profile is shown in Fig. 8. As can be seen, there is good agreement near the hot wall, whereas a small discrepancy is observed near the cool wall (top layer). Given the significant temperature jump at the top layer (11%), this discrepancy had to be expected. The deviations, however, never

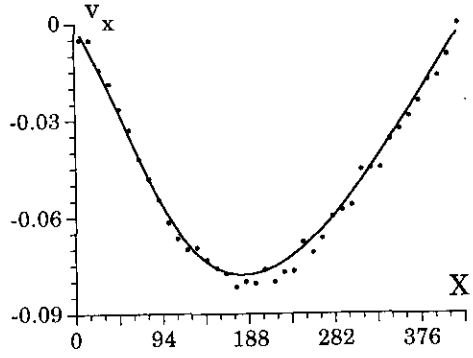

FIG. 7. Velocity profile of the horizontal velocity at ($z = L_z/2$) versus x for Rayleigh–Bénard convection. Solid circles are from Bird simulation with $S_c = 10$; solid line represents the solution of hydrodynamic equations.

exceed 3%, which is well within the expected statistical errors (8%).

6. COMPUTATIONAL EFFICIENCY

The analysis of the previous sections has shown that the enhanced-relaxation variant of the DSMC is in quantitative agreement with equilibrium statistical mechanics and non-equilibrium hydrodynamics. One important question remains: What are the advantages of using this new algorithm for the study of hydrodynamic instabilities, as compared with other computational methods? As was already discussed in the Introduction, we are mainly interested in studying statistical properties of the fluid, so we only consider methods which preserve the correct fluctuation spectrum. For this reason, we exclude from this discussion continuum methods, such as Navier–Stokes solvers, and lattice Boltzmann models. Instead, we compare the efficiency of the enhanced-relaxation DSMC with a hard disk molecular dynamics simulation, in terms of CPU time.

As a specific example, we consider the problem studied in the previous section, a two-dimensional Rayleigh–Bénard

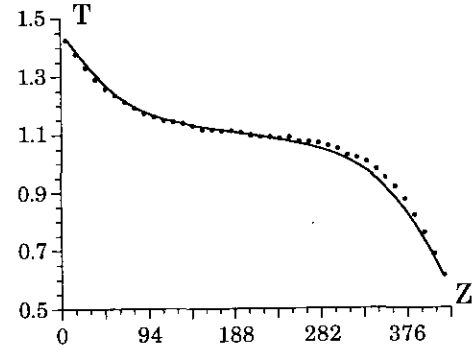

FIG. 8. Vertical temperature profile at ($x = L_x/2$) versus z for Rayleigh–Bénard convection. Solid circles are from Bird simulation with $S_c = 10$; solid line represents the solution of hydrodynamic equations. Note the significant temperature jump, especially at the lower wall.

instability at a prescribed Rayleigh number. Once we fix the temperature difference and use the relation (12) to set the acceleration field g, then the only remaining free parameter is the number density.

It is well known that for hard disk fluids the transport coefficients, that appear in the denominator of the Rayleigh number (11), depend significantly on the number density [27]. This is also the case for the thermal expansion coefficient [28]. A detailed analysis [7] shows that the Rayleigh number has a rather pronounced maximum for values of number density ranging between 0.1 and 0.4 (in system units). For hard disk dynamics, the number density has to be chosen in this range, say 0.2. On the other hand, for the Boltzmann simulation the gas must remain dilute so that the number density cannot exceed 6×10^{-3}, as discussed in the Introduction. We will take the number density to be 5.34×10^{-3}, that is, the value already used in previous sections.

The CPU time of a simulation is directly related to the characteristic time scale for the relaxation processes of hydrodynamical modes. One may consider, for example, the thermal diffusion time $\tau_{\text{diff}} = L_z^2/2\lambda_T$ which represents the time needed for a heat mode to cross the system. During this time, the number of collisions in a system made up of N hard disks is [29]

$$Z_{\text{HD}} = \bar{n} N_{\text{HD}} \tau_{\text{diff}} \chi \sqrt{\pi k_B \bar{T}}, \tag{14}$$

where $\bar{n}$ is the global number density and χ is the pair correlation function at contact [27]. Clearly, the CPU time of a hard disk molecular dynamics simulation will be proportional to Z_{HD}.

For the purpose of comparison, it is useful to write Z_{HD} in terms of the Rayleigh number. Using the relation (12), and the *thermodynamic relation*

$$\frac{T}{\rho^2}\frac{(\partial p/\partial T)_\rho^2}{(\partial p/\partial \rho)_T} = c_p - c_v, \tag{15}$$

the Rayleigh number may be written as

$$R_a = \frac{c_p - c_v}{T}\frac{\Delta T^2 L_z^2}{\nu \lambda_T}. \tag{16}$$

Noting that for hard disk systems the total number of particles is related to the number density through $N_{\text{HD}} = L_z^2 \bar{n}$ (recall that $L_z = L_x$), using the explicit form of the equation of state and transport coefficients [27, 28] and taking $\bar{T} = \Delta T = 1$, one finally obtains

$$Z_{\text{HD}} = 1.02\, R_a^2 \tag{17a}$$

$$N_{\text{HD}} = 2.62\, R_a \approx 2.6 \sqrt{Z_{\text{HD}}}. \tag{17b}$$

Proceeding along the same lines, one may estimate the CPU time for a DSMC simulation. The number of collisions in a

dilute hard-sphere system during a thermal relaxation time, τ_{diff}, is $Z_B = 2\bar{n} N_B \tau_{\text{diff}} \sqrt{\pi k_B \bar{T}}$. The total number of particles, N_B, and the number density, are related through $N_B = L_y L_z^2 \bar{n}$. The simulation is three-dimensional but very shallow in the y direction (i.e., $L_y \ll L_x, L_z$). However, due to the homogeneity assumption made in the construction of the collisional algorithm, L_y cannot be made arbitrarily small. It is well known that the accuracy of the DSMC method is directly related to the average number of particles contained in collisional cells. In general, this number should not be less than 20, since otherwise the local thermalization becomes inefficient and the algorithm gives incorrect transport coefficients [10].

As was already mentioned, the linear dimension of collisional cells must be a fraction of a mean-free path λ. A good choice is to set this linear dimension to half a mean-free path, in which case, using 20 particles per cell, the total number of particles is

$$N_B = 20 \left(\frac{L_z}{\lambda/2} \right)^2. \tag{18}$$

Note that this relation fixes the value of L_y.

Using the explicit form of the transport coefficients for a dilute gas, one finds

$$\frac{Z_B}{Z_{HD}} \approx 38 \tag{19a}$$

$$\frac{N_B}{N_{HD}} \approx 48. \tag{19b}$$

The relation (19a) shows that the hard-disk simulation requires about 40 times fewer collisions than DSMC per relaxation period. It is generally accepted that, per collision, DSMC runs about three orders of magnitude faster than molecular dynamics. Thus, it simulates Rayleigh–Bénard convection nearly two orders of magnitude faster than the corresponding hard-disk dynamics. However, one needs about 50 times more particles.

Let us now consider our enhanced-relaxation variant of DSMC. As we increase the parameter S_c we find that fewer and fewer particles are needed per collisional cell. Surprisingly, we found that for two- or three-dimensional flows, the simulation gives accurate results with one particle per collisional cell when $S_c > 8$. This result was demonstrated in the two-dimensional Rayleigh–Bénard simulations presented in the previous section. For one-dimensional flows, however, we observe that the required minimum number of particles per collisional cell is larger (approximately five for the simulations described in Sections 3 and 4).

Since the "effective" mean-free path is now λ/S_c, the total number of particle N_{ERB} for the enhanced-relaxation Bird algorithm is related to L_z through

$$N_{\text{ERB}} = S_c^2 \left(\frac{L_z}{\lambda/2} \right)^2; \quad S_c \geq 10. \tag{20}$$

Using this result, one easily finds that

$$\frac{Z_{\text{ERB}}}{Z_{HD}} \approx \frac{2}{S_c} \tag{21a}$$

$$\frac{N_{\text{ERB}}}{N_{HD}} \approx 2.4. \tag{21b}$$

Since we take $S_c \geq 10$, we see that the enhanced-relaxation DSMC requires *fewer* collisions than the corresponding hard disk dynamics. But, as discussed in Section 2, the algorithm requires S_c times more CPU per time step than the traditional Bird algorithm. Taking this into account, we still find that the enhanced-relaxation DSMC runs almost three orders of magnitude faster than the corresponding hard disk dynamics yet requires only 2.4 times as many particles!

These impressive results fully justify the use of the enhanced-relaxation DSMC for the study of two-dimensional high Rayleigh number flows. The situation is, however, less promising for high Reynolds number flows. Since, in general, we are interested in strictly sub-sonic flows, the Reynolds number is limited by

$$Re = \frac{C_s L_y}{\nu}, \tag{22}$$

where C_s and L_y are the sound speed and the characteristic length scale, respectively. The sound speed is an increasing function of the density, so that for fixed L_y the Reynolds number is maximum for $\bar{n} \approx 0.78$. On the other hand, the maximum performance for hard-disk dynamics is obtained when the number of collisions during the hydrodynamic relaxation time is minimum. For Poiseuille flow, the relaxation time may be taken as the viscous time $\tau_\nu = L_y^2/2\nu$. For a given prescribed Reynolds number, proceeding as for the Rayleigh–Bénard case, one easily finds that the number of collisions during the relaxation time is

$$Z_{HD} = \frac{Re^4 \nu^3 \bar{n}^2 \chi \sqrt{\pi k_B \bar{T}}}{2 C_s^4}. \tag{23}$$

Figure 9 shows Z_{HD} as a function of the number density. As can be seen the optimal performance for hard-disk dynamics is obtained for $\bar{n} \approx 0.48$. For this density, the sound speed is about 2.5 times larger than in a dilute gas.

Repeating the above calculation for DSMC, we find that it uses about the same CPU time as hard-disk dynamics, yet requires over 400 times more particles, which in turn may become a serious handicap in simulating large Reynolds number flows. The enhanced-relaxation DSMC, on the other hand, runs nearly two orders of magnitude faster and requires about 20

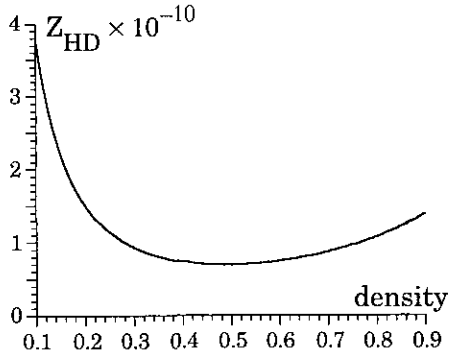

FIG. 9. Total number of collisions per relaxation time as a function of number density for a hard disk molecular dynamics simulation.

times more particles. While the overall performance of the enhanced-relaxation DSMC is not as good as in the Rayleigh–Bénard case, it is still largely competitive with hard-disk dynamics.

Note, finally, that in this section the discussion has been concentrated on two-dimensional systems. In principle, one might expect better performances for the enhanced-relaxation DSMC in three-dimensional cases, since now $N = L_c^3 \bar{n}$. In practice, however, we are limited by the fact that one needs at least one particle, on average, per collisional cell, as we increase the parameter S_c. Explicit calculations, along the same lines as those presented for two-dimensional systems, indicate that the relative performance of the enhanced-relaxation DSMC remains roughly the same for three-dimensional systems, as compared with hard-sphere dynamics.

7. CONCLUSIONS AND PERSPECTIVES

In this paper, we have presented a simple extension of the DSMC method for the simulation of dilute gases. By enhancing the collisional relaxation processes, we were able to significantly reduce the transport coefficients. We established a series of computer experiments which showed that the equilibrium statistical mechanical properties and the hydrodynamic properties of the fluid are correctly reproduced. Furthermore, the computational efficiency of the enhanced-relaxation DSMC was compared with hard-disk dynamics for complex hydrodynamical flows. Our method is ideally suited for the simulation of Rayleigh–Bénard convection, since it is about three orders of magnitude faster than molecular dynamics.

For the simulation of shear-induced instabilities, the relative gain is about two orders of magnitude in computational speed. Unfortunately, since the CPU time of the simulation increases as Re^4 (see Eq. (23)) [30], we are still limited to flows with moderate Reynolds number ($\mathrm{Re} \sim 10^2$ in three-dimensional flows). We are presently using the enhanced-relaxation DSMC method to study two-dimensional Kolmogorov flow [31] and have been able to observe the first few instabilities ($\mathrm{Re} \approx 200$) using modest computational resources (RISC workstations).

At this point one may ask "Are there other modifications to the Bird algorithm which would allow us to reach higher Reynolds number?" There are various ways to increase the Reynolds number in a simulation: increase the flow velocity, increase the system size, or decrease the fluid viscosity. Since one is principally interested in sub-sonic problems, the flow velocity is limited by the sound speed. Unfortunately, since the DSMC method is based on the Boltzmann equation, we are restricted to simulating a dilute gas so the speed of sound is fixed by the ideal gas law.

One way to increase the system size is to increase the collisional cell size, holding the number of particles fixed. We know that, as a rule of thumb, collisional cells in the DSMC algorithm should be a fraction of a mean-free path in size. However, numerical experiments indicate that cells as large as two mean-free paths may often give accurate results [32]. One might also obtain better computational efficiency by using some of the new DSMC features, like, for example, the "cell/sub-cell" hierarchy [22, 33]. While these techniques might increase the Reynolds number by one order of magnitude, their applicability still needs to be established.

A second way to increase system size is to increase the number of collisional cells, holding their size fixed. This will decrease the average number of particles per cell since we fix the total number of particles. The standard DSMC method is accurate when the number of particles per cell is about 20 or more. Surprisingly, the enhanced-relaxation method is often accurate with an average of one particle per collisional cell. These statements are purely observational and not well understood. We are analyzing the algorithm using the theory of Markov processes in an attempt to explain these results. Further study may indicate new ways to modify the collisional algorithm to further reduce the average number of particles per cell.

Finally, one may increase the Reynolds number by finding other ways of lowering the transport coefficients. One of the authors (A.G.) has been experimenting with variants of the hard-sphere collision rules. Conservation of momentum and energy fix four of the six variables in the post-collision velocities. Specifically, the center-of-mass velocity and the magnitude of the relative velocity are unchanged by the collision. In the DSMC algorithm, the direction of the relative velocity is chosen at random; for hard spheres its direction is uniformly distributed over the unit sphere. An alternative collision rule, called the $\times$-rule, is to set the pre- and post-collision relative velocities perpendicular to each other (with the remaining angle uniformly distributed in $[0, 2\pi]$). Preliminary computer experiments indicate that this rule can lower viscosity by about 20–30% while preserving the correct hydrodynamics. Collision rules which violate detailed balance have also been tested and found to dramatically reduce the transport coefficients. Unfortunately, they also produce unphysical artefacts in the flows [34]. Still, it may be expected that the various ideas presented in this section, combined with the enhanced-relaxation DSMC algo-

rithm, will eventually lead to new ways of efficient simulation of high Reynolds number flows at the microscopic level.

ACKNOWLEDGMENTS

The authors wish to acknowledge Drs. G. Nicolis and J. W. Turner for helpful discussions. This work has been supported in part by the Belgian program on inter-university attraction poles. The computing time was allocated through a grant of the Belgian Government (Program "Technologies de l'Information" of SPPS, Contract IT/SC 27) and thanks to the support of the FNRS (supercomputer grant S-6/5-DD-SU.3).

REFERENCES

1. W. G. Hoover, *Computational Statistical Mechanics* (Elsevier Sci., Amsterdam, 1991); D. J. Evans and G. P. Morriss, *Statistical Mechanics of Non-equilibrium Liquids,* (Academic Press, New York, 1990).
2. M. Mareschal (Ed.), *Microscopic Simulation of Complex Flows,* NATO ASI Series, Vol. 236 (Plenum, New York, 1990).
3. M. Mareschal and B. L. Holian (Eds.), *Microscopic Simulations of Complex Hydrodynamic Phenomena,* NATO ASI Series, Vol. 292 (Plenum, New York, 1992).
4. W. G. Hoover, *Phys. Rev. Lett.* **42,** 1531 (1979); B. L. Holian, W. G. Hoover, B. Moran, and G. K. Straub, *Phys. Rev. A* **22,** 2798 (1980); B. L. Holian, *Phys. Rev. A* **37,** 2562 (1988).
5. D. C. Rapaport and E. Clementi, *Phys. Rev. Lett.* **57,** 695 (1987); L. Hannon, G. Lie, and E. Clementi, *J. Sci. Comput.* **1,** 145 (1986); D. C. Rapaport, *Phys. Rev. A* **36,** 3288 (1987); E. Meiburg, *Phys. Fluids* **29,** 3107 (1986).
6. M. Mareschal and E. Kestemont, *Nature* **323,** 427 (1987); *J. Stat. Phys.* **48,** 1187 (1987); D. C. Rapaport, *Phys. Rev. Lett.* **60,** 2480 (1988).
7. M. Mareschal, M. Malek Mansour, A. Puhl, and E. Kestemont, *Phys. Rev. Lett.* **61,** 2550 (1988); A. Puhl, M. Malek Mansour, and M. Mareschal, *Phys. Rev. A* **40,** 1999 (1989).
8. U. Frisch and S. Orzag, *Physics Today,* January 1990, p. 24.
9. D. C. Rapaport, *Phys. Rev. A* **43,** 7046 (1991); **46,** (1992).
10. G. A. Bird, *Molecular Gas Dynamics* (Clarendon, Oxford, 1976).
11. See, for example, S. Succi, R. Benzi, A. Cali, and M. Vergassola, in [3, p. 187]; C. Burges and S. Zaleski, *Complex Systems* **1,** 31 (1987); D. H. Rothman, in [3, p. 221].
12. G. McNamara and B. Alder's, Ref. [3].
13. D. Dab, A. Lawniczak, J. P. Boon, and R. Kapral, *Phys. Rev. Lett.* **64,** 2462 (1990); D. Dab, J. P. Boon, and Y. Li, *Phys. Rev. Lett.* **66,** 2535 (1991); R. Kapral, A. Lawniczak, and P. Masiar, *Phys. Rev. Lett.* **66,** 2539 (1991).
14. For a recent review, see M. Nelkin, *Science* **255,** 566 (1992).
15. Recently, however, it has been shown that LGCA reproduces correctly the dynamic of the density fluctuations in an equilibrium system: P. Grosfils, J. P. Boon, and P. Lallemand, *Phys. Rev. Lett.* **68,** 1077 (1992); P. Grosfils, J. P. Boon, R. Brito, and M. H. Ernst, *Phys. Rev. E* **48,** 2665 (1993). A lattice Boltzmann simulation with fluctuating stress tensor (Landau–Lifshitz) is presented in A. J. C. Ladd, *Phys. Rev. Lett.* **70,** 1339 (1993).
16. M. Malek Mansour, A. Garcia, G. Lie, and E. Clementi, *Phys. Rev. Lett.* **58,** 874 (1987); A. Garcia, M. Malek Mansour, G. Lie, and E. Clementi, *Phys. Rev. A* **36,** 4348 (1987).
17. E. Salomons and M. Mareschal, *Phys. Rev. Lett.* **69,** 269 (1992).
18. L. C. Landau and E. M. Lifshitz, *Fluid Mechanics* (Pergamon, Oxford, 1984).
19. M. Kac, in *Probability Theory and Related Topics in Physical Science* (Wiley, New York, 1959); J. Logan and M. Kac, *Phys. Rev. A* **13,** 458 (1976); A. Onuki, *J. Stat. Phys.* **18,** 475 (1978); L. Brenig and C. Van den Broeck, *Phys. Rev. A* **21,** 1039 (1980).
20. W. Wagner, *J. Stat. Phys.* **66,** 1011 (1992).
21. P. Résibois and M. De Leener, *Classical Kinetic Theory of Fluids,* (Plenum, New York, 1976).
22. G. A. Bird, *Molecular Gas Dynamics and the Direct Simulation of Gas Flows* (Clarendon, Oxford, 1994).
23. L. Hannon, G. Lie, and E. Clementi, *Phys. Lett. A* **119,** 174 (1986).
24. C. Cercignani, *Mathematical Methods in Kinetic Theory* (Plenum, New York, 1990); D. Morris, L. Hannon, and A. Garcia, *Phys. Rev. A* **46,** 5279 (1992).
25. B. J. Berne and R. Pecora, *Dynamic Light Scattering* (Wiley, New York, 1976); J. P. Boon and S. Yip, *Molecular Hydrodynamics* (McGraw–Hill, New York, 1980).
26. S. Chandrasekhar, *Hydrodynamic and Hydromagnetic Stability* (Clarendon, Oxford, 1961).
27. D. M. Gass, *J. Chem. Phys.* **54,** 1898 (1971).
28. J. A. Barker and D. E. Henderson, *Rev. Mod. Phys.* **48,** 587 (1976).
29. S. Chapman and T. G. Cowling, *The Mathematical Theory of Non-uniform Gases* (Cambridge Univ. Press, Cambridge, 1960).
30. Note that at very high Reynolds number, due to turbulent mixing, the computation time goes as Re^{α}, where $3 < \alpha < 4$.
31. M. Mareschal and P. Peeters, preprint.
32. D. Baganoff, private communication.
33. G. A. Bird, Ref. [3, p. 239].
34. B. Alder, K. Siegel, and A. Garcia, to be published.